

UC Irvine

UC Irvine Previously Published Works

Title

Synergistic reaction of silver nitrate, silver nanoparticles, and methylene blue against bacteria

Permalink

<https://escholarship.org/uc/item/2tt8f6d9>

Journal

Proceedings of the National Academy of Sciences of the United States of America, 113(48)

ISSN

0027-8424

Authors

Li, Runze
Chen, Jie
Cesario, Thomas C
et al.

Publication Date

2016-11-29

DOI

10.1073/pnas.1611193113

Peer reviewed

Synergistic reaction of silver nitrate, silver nanoparticles, and methylene blue against bacteria

Runze Li^a, Jie Chen^{b,c}, Thomas C. Cesario^d, Xin Wang^e, Joshua S. Yuan^e, and Peter M. Rentzepis^{a,1}

^aDepartment of Electrical and Computer Engineering, Texas A&M University, College Station, TX 77843; ^bDepartment of Physics and Astronomy, Key Laboratory for Laser Plasmas (Ministry of Education), Shanghai Jiao Tong University, Shanghai 200240, China; ^cCollaborative Innovation Center of Inertial Fusion Sciences and Applications (CICIFSA), Shanghai Jiao Tong University, Shanghai 200240, China; ^dDepartment of Medicine, University of California, Irvine, CA 92697; and ^eDepartment of Plant Pathology and Microbiology, Texas A&M University, College Station, TX 77843

Contributed by Peter M. Rentzepis, August 31, 2016 (sent for review July 11, 2016; reviewed by Sadik C. Esener and Ting Guo)

In this paper we describe the antibacterial effect of methylene blue, MB, and silver nitrate reacting alone and in combination against five bacterial strains including *Serratia marcescens* and *Escherichia coli* bacteria. The data presented suggest that when the two components are combined and react together against bacteria, the effects can be up to three orders of magnitude greater than that of the sum of the two components reacting alone against bacteria. Analysis of the experimental data provides proof that a synergistic mechanism is operative within a dose range when the two components react together, and additive when reacting alone against bacteria.

bacteria | synergistic effect | methylene blue | silver ions

Bacterial infections cause countless deaths in humans and animals. The increasing resistance and immunity of many bacteria to antibiotics demands that an effective means for the inactivation of bacteria becomes available that can overcome or negate the mechanism that bacteria use to inactivate the reactive agents before they render their lethal action on those organisms. The two antibacterial agents that we used in this study were methylene blue (MB) and silver nitrate. Each of these alone is known to be an effective antibacterial agent. The data presented in this study show that they make a synergistic agent pair against the five bacteria studied. MB is used as a bacterial inactivator for skin treatment, dental therapy, and other areas in need of bacterial disinfection (1–3). MB is a cation, whereas in its reduced leuco form MB has a pK_a of 5.8 and low ionization at neutral physiological pH. This enables bacteria to reduce and inactivate MB to the leuco form. In fact, the discoloration of MB has been an indication of the presence of bacteria. In its cationic form, MB irradiated with 630–680-nm light is used for cancer therapy and as an effective bactericidal and activating agent. MB is an effective antibacterial agent owing to its ability to generate a high concentration of singlet oxygen, 1O_2 ($^1\Delta_g$), and other reactive oxygen species, such as OH^\bullet radicals (ROS), when irradiated with red light, which in contrast to UV light does not harm humans or animals cells. Therefore, the MB bacterial inactivation process is very safe and effective owing to the high reactivity of ROS with bacterial outer-cell membrane. It is found that the photogenerated singlet oxygen reacts against tryptophan and other outer-membrane molecules, resulting in damage to the bacterial cell and inhibiting protein production. ROS may also create a hole in the bacterial cell wall, which allows MB radicals to penetrate through the bacterial membrane and attack DNA, forming dimers which prevent it from replicating and consequently induce bacterial inactivation. The photoreaction that generates singlet oxygen and OH^\bullet radicals proceeds as follows:

- i) MB in water solution is excited to the first singlet state MB^* :
 $MB + h\nu$ (660 nm) $\rightarrow MB^*$;
- ii) MB^* decays to the triplet state $^3MB^*$ with a lifetime of $\sim 10^{-9}$ s:
 $MB^* \rightarrow ^3MB^*$;
- iii) The triplet $^3MB^*$ transfers electrons, Rxn type I, or energy, Rxn type II, to the ground-state molecular, triple-state oxygen, 3O_2 forming OH^\bullet radicals and singlet oxygen, 1O_2 ($^1\Delta_g$):
 $^3MB^* + O_2 \rightarrow ^1O_2$.

Both of these reactive species 1O_2 ($^1\Delta_g$) and OH^\bullet radicals formed by energy transfer, type I and electron transfer, type II, respectively, have very short reactive mean-free paths of 100 Å and 10 Å, respectively (4, 5), which place a limit on the maximum distance between MB and bacteria for the ROS to be effective agents against bacteria. Positively charged photosensitizers are expected to be more effective bacterial inactivators than neutral molecules against Gram-negative bacteria, whose outer membranes are composed of negatively charged lipopolysaccharides. In contrast, Gram-positive bacteria may be inactivated more effectively by neutral or negatively charged agents. The MB photo-generated singlet oxygen reacts with the bacteria components including proteins and even DNA after penetrating the cell through the openings generated by the singlet-oxygen oxidation of the wall membrane. Singlet oxygen is also thought to be the dominant biocidal agent by oxidizing phospholipids, peptides, and tryptophan, which are essential for bacteria replication. Also, $^3MB^*$ undergoes electron transfer, type II reaction with cytoplasm to form OH^\bullet radicals that react with pathogens, resulting in toxic inactivation. As much as a wide range of bacteria has been found to be susceptible to MB photodynamic therapy (PDT), no experimental evidence has been published which suggests the existence of bacteria resistant to MB PDT (6).

The second agent of this study, silver nitrate ($AgNO_3$), has been used as an antibacterial agent in the form of metallic silver since ancient times. Later, in the 1800s, dilute silver nitrate was used to prevent the transmission of *Neisseria gonorrhoeae* to newborn infants and prevent infections (7, 8), and silver-coated dressings have also been used to treat wounds and dental infections (9, 10). The antibacterial effect of silver ions and silver nanoparticles,

Significance

Bacteria are increasingly becoming resistant to antibiotics; therefore, other means must be found for their inactivation. Efficient inactivation of bacteria cannot be achieved simply by increasing the dose because of toxicity limitation. Therefore, it is critical to search for a combination of agents, within a safe dose, that is more effective in killing bacteria than agents reacting alone. Here, we show that the combination of methylene blue (MB) and silver nitrate can be up to three orders of magnitude more effective in killing bacteria than the two agents reacting alone against bacteria. This synergistic mechanism is due to silver ion increasing the penetration of MB into the bacteria interior, allowing photogenerated single oxygen to react with DNA and prevent replication.

Author contributions: T.C.C. and P.M.R. designed research; R.L., J.C., T.C.C., X.W., J.S.Y., and P.M.R. performed research; R.L., J.C., T.C.C., X.W., J.S.Y., and P.M.R. contributed new reagents/analytic tools; R.L., T.C.C., and P.M.R. analyzed data; and R.L., T.C.C., and P.M.R. wrote the paper.

Reviewers: S.C.E., University of California, San Diego; T.G., University of California, Davis.

The authors declare no conflict of interest.

¹To whom correspondence should be addressed. Email: prentzepis@tamu.edu.

This article contains supporting information online at www.pnas.org/lookup/suppl/doi:10.1073/pnas.1611193113/-DCSupplemental.

AgNPs, on Gram-positive bacteria, which are a major cause of hospital infections, and on Gram-negative bacteria has been studied extensively (11). A main advantage of the use of silver nitrate and silver compounds in general, for antibacterial infections, is the fact that Ag^+ is relatively nontoxic to human and animal cells, and in addition is very effective against fungi and viruses. It has been reported (12) that silver nitrate kills bacteria at higher concentrations than AgNPs, whereas SEM and X-ray diffraction data have shown that at lower silver nitrate concentrations bacteria may synthesize nanoparticles (13, 14). Even though the reaction of Ag^+ ions with bacteria has been studied in depth for long periods of time, the inactivation mechanism is not entirely known and the reaction of nanoparticles with these pathogens is even less well understood (15). Ag^+ ions are thought to attack the DNA thiol bases, forming dimers that prevent DNA replication. AgNP and silver metal in water solutions release silver in the form of Ag^+ ions, which act as antibacterial agents in the same manner as AgNO_3 . Therefore, the reaction of these three species against bacteria is believed to be essentially the same, although the rate of inactivation may vary widely, most probably owing to the rate of Ag^+ release. It has also been known, for a rather long time, that Ag^+ ions bind to thiol groups containing cell membranes and enzymes, forming stable S–Ag bonds (16), denature them, and thus prevent DNA replication by condensation (17, 18). Silver is also involved in catalytic oxidation reactions that form R–S–S–R disulfides, which are achieved by silver catalyzing the reaction between the oxygen dissolved in the cell and the hydrogen of the S–H thiol group (19).

Ag^+ ions, in concentration of parts per billion, have been known to react with maltose transporter and fructose biphosphate aldolase protein, causing expression decrease (20, 21). Treatment with Ag^+ has been found to degrade several proteins and associate with the bacterial DNA after it penetrates the cell wall (22). To that effect, we find that Ag^+ enters the bacterial cell and intercalates between the base pair of purine and pyrimidine, thus disrupting H bonding between antiparallel strands, causing the denaturation of DNA and the subsequent inactivation of bacterial. Our data suggest, as most investigators believe, that Ag should be in its ionic form, Ag^+ , to be an effective antibacterial agent and that silver in its metallic nonion form is rather inert (23–25). Silver ions and the MB-induced ROS penetrate bacterial cells through their hydrophobic membrane to access the cytoplasm. One such pathway is the transmembrane protein that normally transports ions other than Ag^+ . However, *Enterococcus hirae* proteins are known to transport silver ions (26). Using these two agents, MB and AgNO_3 , to react together against bacteria, we find that a synergistic effect occurs which is thousands of times more effective in killing bacteria than the two agents reacting alone. Experiments in vivo and in vitro suggested that Ag^+ disrupts disulfide bond formation in proteins, which is expected to contribute to protein misfolding and aggregation. Ag^+ also interacts with bacteria and disrupts Fe–S clusters. In addition, it generates superoxide formations, which cause Fe^{2+} leakage. These alterations in cellular morphology increase outer-membrane permeability, which allows ROS and possibly MB to penetrate through the membrane wall and cause bacterial inactivation. The Ag^+ and MB doses that we used have been found to be well tolerated by mice (27), whereas the therapeutic index of Ag^+ has been calculated to vary between 8~16, which is within the range of the therapeutic doses approved for Food and Drug Administration antibiotics. Ag^+ was found previously to have a synergistic effect against bacteria when used in combination with β -lactam (27), enhancing the ability of Ag^+ to induce permeability in the bacterial outer membrane.

Synergism

Many biocidal agents are not as effective against pathogens as one would expect, or want, because the dose is often toxicity limited. Therefore, as a means for increasing the biocidal effects of agents while using small doses, one searches for a synergistic combination

that is more effective than the sum of its individual components acting alone. A rather simple and accurate procedure that makes it possible to compare the effectiveness of different agents against bacteria is to determine the concentration or dose of each constituent that produces the same quantitative effect when used alone. Then, compare it with the effect of the two agents reacting together, under the same conditions, against the same number of bacteria. For example, for the case of two bacterial-killing agents, one determines the concentration of agent A and then agent B, which kills the same number of bacteria and generates a plot (isobole) of these data. Such a plot (28), shown in Fig. 1, depicts clearly the effect of each component A and B alone and the effect of A and B components when used together. The shape of the resulting line provides a clear indication whether the effect is additive, straight line; antagonistic, convex curve; or synergistic, concave curve.

Another method that we have used in this study to determine the type of effect that is operative was to measure the number of bacteria remaining alive after the dose of each component, $f(a)$ and $f(b)$, alone and in combination, $f(a + b)$ (28, 29). The effect is synergistic when the sum of two components, $f(a + b)$, reacting together against bacteria, left a smaller number of bacteria alive than the sum of the two components $f(a) + f(b)$ reacting alone. To make certain that the true mechanism of the reaction is synergistic, the values of $2f(a)$ and $2f(b)$ should also be determined and compared with the value of $f(a + b)$, and show that $2f(a) > f(a + b)$ and $2f(b) > f(a + b)$. The concept of synergism and the correct means for determining whether the effect is synergistic, additive, or antagonistic has been described in several reviews on this subject (28, 30), and papers on its applications to various agents (31–33), theoretical treatment, and modeling (34–36).

Another important test to determine whether the effect of two reactants is synergistic or not may be provided by the relationship between the doses of the two reactants A and B described by the relationship

$$\frac{\text{Dose of } A}{A_c} + \frac{\text{Dose of } B}{B_c} \begin{cases} < 1, \text{ synergistic} \\ = 1, \text{ additive} \\ > 1, \text{ antagonistic} \end{cases} \quad [1]$$

where A and B are the doses used for components A, B; and A_c and B_c are the doses of A and B that result in the same quantitative

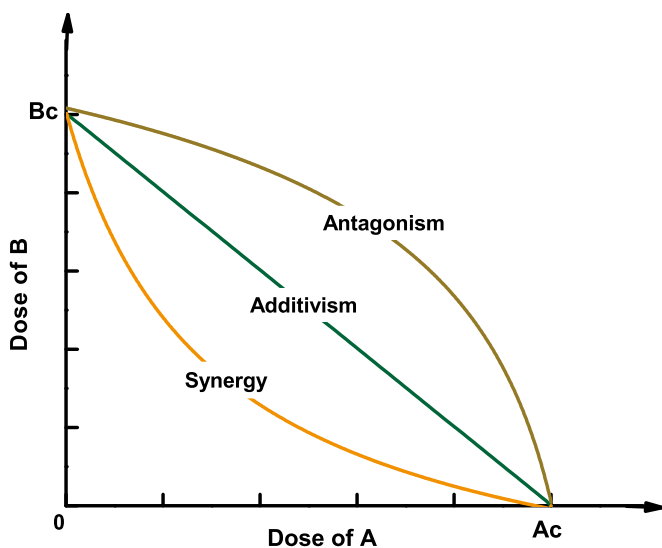


Fig. 1. Isoboles for synergistic, additive, and antagonistic effects. A_c and B_c are doses of reactant A and reactant B that produce an equal effect. The isoboles are lines that connect points of equal effect (28).

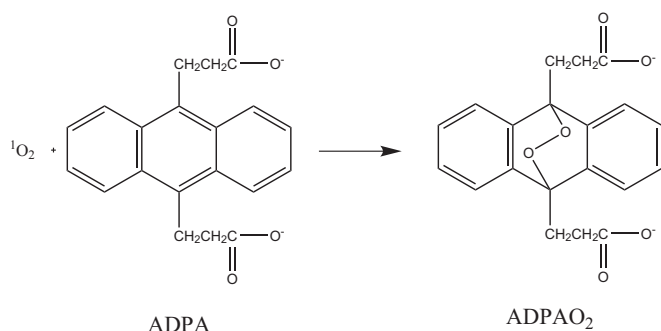
effect, i.e., the same number of live bacteria. If the sum of these two fractions is = 1, then the effect is additive and becomes synergistic or antagonistic if the sum of the fractions is <1, or >1, respectively (37). A further means for deciding if the effect is synergistic is to determine if the concentration of each antibacterial agent, in the combination that generates the specific effect, is a fraction of the concentration that produces the same effect when the antibacterial agent is used alone, namely determine the fractional inhibitory concentration (FIC) (29).

Experimental

Assessing the agent combination that allows for the determination of synergy is quantitative study that requires the determination of the individual dose(s) from which the combined and individual effect is calculated and determined. We performed a number of experiments using several doses, concentration of MB, AgNO₃, and AgNP, to determine their efficacy in killing bacteria alone and in combination with each other. Then, we used these data to determine if the effect is synergistic or not using the fractional and geometric isobole methods. First, we ascertained that neither AgNO₃ nor silver nanoparticles, AgNP, when irradiated with 660-nm light-emitting diode (LED), generated ROS, which may influence their reaction against bacteria either alone or in combination with MB. The yield of singlet oxygen was measured by monitoring the decrease of the 399-nm absorption band of anthracene dipropionic acid salt (ADPA), a typical probe for singlet-oxygen detection (38).

Scheme 1 shows the reaction of singlet oxygen with dipropionic acid. It is noted that this reaction is unique to singlet oxygen and that dipropionic acid does not react with ground-state molecular oxygen. The amount of singlet oxygen formed is determined by the magnitude of the slope of the reaction of ADPA, OD vs. time, exclusively with singlet-oxygen. The data displayed in Fig. 2 show clearly that the ADPA slope in the AgNO₃ and AgNP solutions is practically zero. Therefore, as stated above, no observable singlet oxygen was produced by the photolysis of these silver agents. In contrast, the ADPA slope is 0.029 and 0.022 in MB and equal amounts MB + AgNO₃ solutions, respectively. As expected, this figure proves that ¹O₂ is generated by MB only. Therefore, the inhibiting reaction of AgNO₃ and AgNP against bacteria is not due to photogenerated singlet oxygen or ROS, as is the case with MB.

Experiments were conducted with five different bacteria: *S. marcescens* (SM), *Escherichia coli*, *Klebsiella pneumoniae* (KP), *Pseudomonas aeruginosa* (PA), and *Enterobacter cloacae* (EC), into which we added: (a) MB alone; (b) AgNO₃ alone; (c) AgNP alone; (d) MB + AgNO₃; and (e) MB + AgNP, and determined the biocidal effect of each of these agents alone, (a), (b), (c) and in combination, (d), (e) against bacterial strain, while being irradiated with 660-nm, 6.8-mW LED for 180 min. Subsequently, the numbers of live bacteria were determined by the normal 24-h incubation method and enumeration of bacteria colony-forming units (CFUs). The number of bacteria is referred to as "logs,"



Scheme 1. Reaction of ADPA with singlet oxygen.

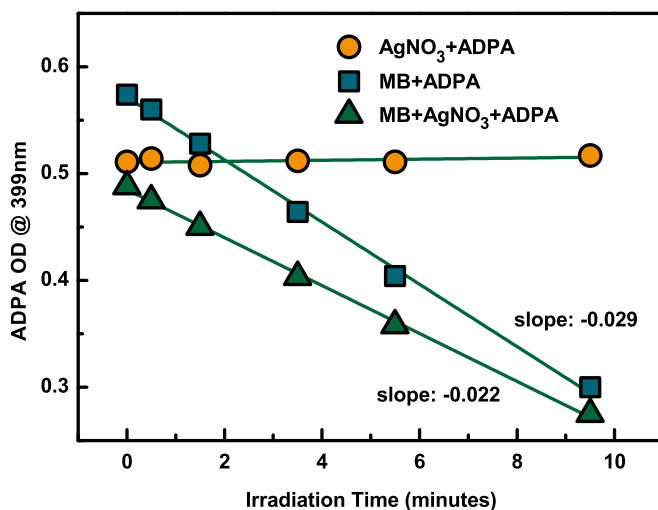


Fig. 2. Amount of singlet oxygen generated by each molecule: AgNO₃ and MB alone and both combined after illumination with 6.8-mW, 660-nm LED light.

which equals log₁₀. The experimental data are listed in Table 1. It is evident from those data that the number of live bacteria remaining after the combined reaction of the two agents against bacteria is always smaller than the number of live bacteria remaining after the sum of the two agents reacting alone against an equal number of the same bacteria.

Fig. 3 shows the effect of the two agents acting alone and in combination against the five bacteria studied. Fig. 3A shows the synergistic effect of MB and AgNO₃ against SM, *E. coli*, KP, PA, and EC. Fig. 3B shows the synergistic effect on two different bacterial concentrations. Fig. 3C shows that when using two different concentration of AgNO₃, 7.75 μg/mL and 15.5 μg/mL, the effect is also synergistic; Fig. 3D shows the effect of labeling the MB concentration 20 to 40 μg/mL; the effect of the combined agents against *E. coli* bacteria is larger than the sum of the two components alone.

Our study shows that a synergistic effect is operative for doses ranging from 20 to 40 μg/mL for MB and 7.75 to 15.5 μg/mL for AgNO₃. This AgNO₃ dose is sublethal to mice (27). The data listed in Table 1 show that both 2f(a) and 2f(b) doses left a larger number of live bacteria than f(a + b); therefore, this provides proof that the combined agent effect, f(a + b), is synergistic. The detail experimental results are listed in Table 1. Below we list a set of data recorded in one experiment.

Control: 6.3 logs (2.0 × 10⁶), Control = SM bacteria in plasma; MB = 20 μg/mL (6.2 × 10⁻⁵ M); AgNO₃ = 7.75 μg/mL (7.2 × 10⁻⁵ M):

- i) 20 μg/ml MB + control = 5.6 logs;
Live bacteria: 4.0 × 10⁵ (5.6 logs)
- ii) 7.75 μg/ml AgNO₃ + control = 5.5 logs;
Live bacteria: 3.0 × 10⁵ (5.5 logs)
- iii) 20 μg/ml MB + 7.75 μg/ml AgNO₃ + control = 2.7 logs;
Live bacteria: 5.0 × 10² (2.7 logs)

For the effect to be synergistic, the number of live bacteria after the reaction of the combined agents, f(a + b), must be less than the sum of bacteria left alive after the two agents f(a) + f(b) reacted alone.

Bacteria alive after agent(s) reaction with 2.0 × 10⁶ (6.3 logs) bacteria: f(a) = 4.0 × 10⁵ (5.6 logs), f(b) = 3.0 × 10⁵ (5.5 logs). Therefore, f(a) + f(b) = 7.0 × 10⁵ alive after reacting with 4.0 × 10⁶ bacteria, which corresponds to 3.5 × 10⁵ live bacteria after reacting with 2.0 × 10⁶ bacteria. Similarly, f(a + b) = 5.0 × 10² live after reacting with 2.0 × 10⁶ bacteria. Therefore, f(a + b) << f(a) + f(b) and these data suggest that the reaction of the combined MB and

which means that the effect is synergistic. The isoboles generated by our data show that the effect of the two agents reacting alone against bacteria is additive; in combination the effect is synergistic. Synergism is also the operative mechanism if the concentration of each antibacterial component, in the combination that generates the specific effect, is a fraction of the concentration that produces the same effect when the antibacterial agent is used alone, namely the FIC. In our case, when MB and AgNO₃ are the two components, according to the data listed in Table 1 the sum of these fractions is <1, which provides further confirmation that the effect is synergistic.

We also performed similar experiments with 7.2 logs (1.6×10^7) *E. coli* bacteria [American Type Culture Collection (ATCC) 25922]. In this case the dose $f(a)$ of MB is 20 $\mu\text{g}/\text{mL}$ and the dose $f(b)$ of AgNO₃ is 7.75 $\mu\text{g}/\text{mL}$. When $f(a)$ alone is mixed with *E. coli* and illuminated with the 660-nm LED for 180 min, we find that 8.0×10^5 (5.9 logs) bacteria remain alive, whereas under identical conditions $f(b)$ alone left 4.0×10^6 (6.6 logs) live bacteria. This indicates that $f(a) + f(b) = 2.4 \times 10^6$ alive after reacting with 1.6×10^7 bacteria. In contrast, when the two reagents MB and AgNO₃ are combined, $f(a + b)$, and irradiated together with *E. coli* bacteria we find that 8.0×10^1 (1.9 logs) bacteria remained alive after reacting with 1.6×10^7 bacteria. These data show that $f(a + b) \ll f(a) + f(b)$, the combination of these agents acting together, left fewer live bacteria than the two reagents reacting alone against bacteria. Essentially, 30,000 \times fewer *E. coli* bacteria remain alive by the two agents combined than the sum of the two agents reacting alone with the same concentration of *E. coli* bacteria. An additional means for ascertaining the nature of the effect is provided by substituting into Eq. 1 the corresponding values for MB and AgNO₃ where A_c and B_c are the doses of A and B that result in the same quantitative effect

$$\frac{7.75}{28} + \frac{20}{80} < 1.$$

The <1 value is an indication of synergistic effect. The same types of isobole curves, as shown in Figs. 4 and 5, were plotted using the data listed in Table 1, for doses of 7.75 and 15.5 $\mu\text{g}/\text{mL}$ for AgNO₃, and 10 and 20 $\mu\text{g}/\text{mL}$ for MB, respectively, against SM and *E. coli* bacteria. We find straight isobole lines for each component reacting alone and concave isoboles for the two agents' combined effect. These curves show that the effect of the combined doses is synergistic and the effect of individual components alone is additive. The synergistic effect under different illumination times of the 660-nm LED is shown in Fig. S1.

Although the mechanism for the synergistic effect observed for the combined MB/AgNO₃ reaction of against bacteria is not completely known at the present time, experimental studies in progress suggest that Ag⁺ ions, interacting with the outer membrane of Gram-negative bacteria, generate channels with openings large enough for the MB reagent to penetrate the bacterial wall

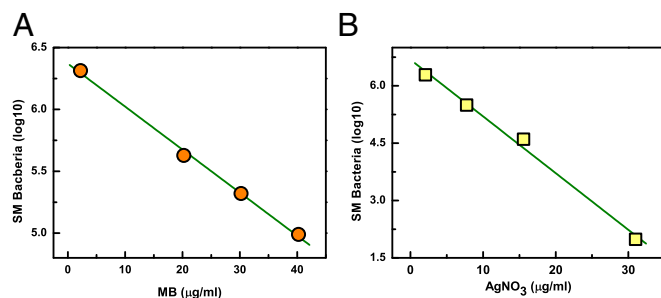


Fig. 4. (A) MB dose vs. SM bacterial killing; (B) AgNO₃ dose vs. SM bacterial killing.

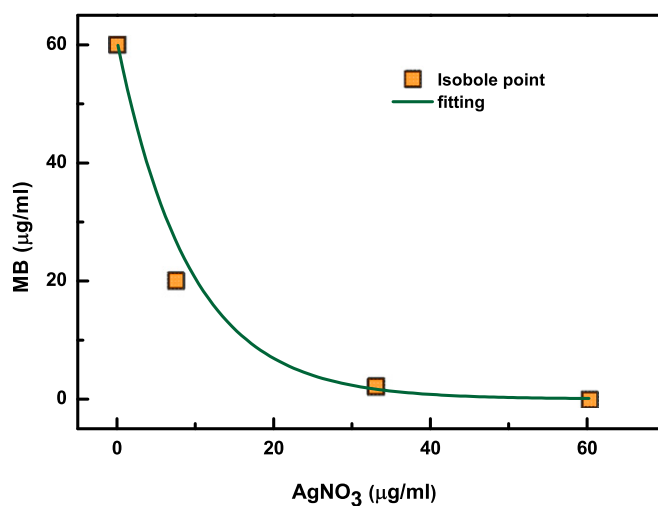


Fig. 5. Isobole plot. Doses of MB and AgNO₃ that have the same effect on SM bacteria.

and enter the interior of the cell. This enables the MB photo-generated singlet oxygen, OH[•] radicals, and MB radicals to be in contact and react directly with bacterial components including tryptophan and oxidize it, thus inhibiting protein formation and even forming DNA dimers which prevent bacterial replication. There is a possibility of peroxide formation which will also react with the bacterial membrane. This process enhances, several-fold, the effectiveness of MB against Gram-negative bacteria and partly explain the observed AgNO₃/MB synergistic effect. Our preliminary experimental data and previously published results (27) indicate that a major factor for the observed synergistic effect is the ability of silver ions to interact with the outer membrane of Gram-negative bacteria and increase its permeability to MB, enabling the MB photogenerated ROS to oxidize several bacterial components including DNA and consequently kill bacteria with high efficacy. We are studying these and other reactions to determine the mechanism(s) responsible for the observed synergetic effect of silver ions and nanoparticles in conjunction with MB irradiated with the 660-nm red light.

Even though the biocide reactions of silver nitrate and AgNO₃ are well documented, their use as antibacterial agents in open wounds is not widely recommended because there is evidence that high doses of silver ions are harmful to human tissue (39, 40). To understand the toxic effect, if any, that the MB/AgNO₃ synergistic effect has on live tissue, we performed experiments using fetal foreskin fibroblasts.

Fetal foreskin fibroblasts were grown to confluence in 48-well microtiter plates. In parallel, rows on the plate were placed in: (i) plain culture medium, (ii) a solution of AgNO₃ diluted one-to-one in plasma to reach a final concentration of 33 $\mu\text{g}/\text{mL}$, (iii) a solution of AgNO₃ diluted one-to-one in plasma to reach a final concentration of 15.5 $\mu\text{g}/\text{mL}$, (iv) plasma alone, (v) MB diluted one-to-one in plasma to reach a final concentration of 20 $\mu\text{g}/\text{mL}$, (vi) a solution of AgNO₃ at a final concentration of 15.5 $\mu\text{g}/\text{mL}$ with MB at a final concentration of 20 $\mu\text{g}/\text{mL}$ diluted one-to-one in plasma. One half of the plate was covered in aluminum foil and the plate was placed under a red light and excited at 660 nm for 3 h at a temperature of 34 $^{\circ}\text{C}$. The light flux was 6.8 mW. At the completion of the period of irradiation, each well was inspected by light microscopy. The cells on all rows were intact save for those cells exposed to AgNO₃ at 33 $\mu\text{g}/\text{mL}$, which were detached and fragmented. A commercial preparation of trypan blue was then added to two columns of the plate at the appropriate concentration and the cells were again inspected after 15 min and every day thereafter

for 72 h and again at 7 d. All of the cells that remained attached to the bottom of the wells of the plate, including those exposed to the lower concentration of MB and AgNO₃ combined, excluded trypan blue for the entire 7-d observation period and continued to be intact. Thus, the fetal foreskin fibroblasts remained viable after exposure to the MB/AgNO₃ preparations used to kill the bacteria tested here.

These results show that using the doses of our synergistic effect experiments, 20 μg/mL MB and 7.75 μg/mL AgNO₃, the MB/AgNO₃ combination may be used for bacteria inactivation in open wounds and other therapeutic applications.

Conclusion

The data and analysis presented show that when MB and AgNO₃ are combined and react together against five different bacteria, the effect is synergistic, within a dose(s) limit. The number of bacteria that remain alive after the reaction of the combined two agents is about three orders of magnitudes smaller than the sum of the two agents reacting alone against the same number of bacteria. These data allow one to determine the dose combination that is optimal for pathogen inactivation and effective elimination of bacterial infections. Possible application of this antibacterial synergistic system is for the in situ treatment of burn wounds and many other infections, including water disinfection. Fetal foreskin fibroblasts grown to confluence, placed in plasma, MB, AgNO₃,

and MB/AgNO₃ combination and irradiated with 660-nm, 6.8-mW light for 3 h remain viable, suggesting that our MB/AgNO₃ combination may be used effectively in wound therapy.

Materials and Methods

The bacteria presented in this study were purchased from the ATCC Manassas; MB and AgNO₃ were purchased from Sigma-Aldrich and used without further purification; ADPA was purchased from Chemodex and kept refrigerated until use. The absorption spectra of MB and ADPA were measured using a Shimadzu 1600 UV spectrophotometer, in 1-mm optical path-length quartz cells. The concentration of single oxygen, ¹O₂ (¹Δ_g), generated by MB (Fig. 2) was determined by the decrease in the OD of ADPA at 399 nm. The concentration of MB and AgNO₃ solutions, (i) AgNO₃ + ADPA, (ii) MB + ADPA, (iii) AgNO₃ + MB + ADPA, were kept the same for all measurements. The 660-nm, monochromatic LED light was focused onto the cell with a 25-cm lens and the power, 6.8 mW, was measured by a Molectron PM3Q detector. After each irradiation, the absorption spectrum was measured and the OD at 399 nm was plotted vs. irradiation time (Fig. 2). Bacteria were added to PBS or plasma solvents. The number of bacteria was determined by the normal 24-h incubation method, in agar, at 30–37 °C and then counting the CFUs. Fetal foreskin fibroblasts were grown to confluence in 48-well microtiter plates and allowed to react with MB and AgNO₃ combined and inspected by light microscopy.

ACKNOWLEDGMENTS. We thank Dr. Martina Berger for performing the cell experiments. This research was supported by The Welch Foundation, Support Grant 1501928, Texas A&M Engineering Experiment Station, and Texas A&M University.

- Dai T, Huang Y-Y, Hamblin MR (2009) Photodynamic therapy for localized infections—state of the art. *Photodiagn Photodyn Ther* 6(3-4):170–188.
- Zeina B, Greenman J, Purcell WM, Das B (2001) Killing of cutaneous microbial species by photodynamic therapy. *Br J Dermatol* 144(2):274–278.
- Wainwright M (1998) Photodynamic antimicrobial chemotherapy (PACT). *J Antimicrob Chemother* 42(1):13–28.
- Moan J, Berg K (1991) The photodegradation of porphyrins in cells can be used to estimate the lifetime of singlet oxygen. *Photochem Photobiol* 53(4):549–553.
- Pryor WA (1986) Oxy-radicals and related species: Their formation, lifetimes, and reactions. *Annu Rev Physiol* 48:657–667.
- Wainwright M, Crossley KB (2002) Methylene Blue—a therapeutic dye for all seasons? *J Chemother* 14(5):431–443.
- Silvestry-Rodriguez N, et al. (2007) Silver as a disinfectant. *Reviews of Environmental Contamination and Toxicology* (Springer, New York), pp 23–45.
- Russell AD, Hugo WB (1994) Antimicrobial activity and action of silver. *Prog Med Chem* 31:351–370.
- Leaper DJ (2006) Silver dressings: Their role in wound management. *Int Wound J* 3(4):282–294.
- Olson ME, Wright JB, Lam K, Burrell RE (2000) Healing of porcine donor sites covered with silver-coated dressings. *Eur J Surg* 166(6):486–489.
- Holt KB, Bard AJ (2005) Interaction of silver(I) ions with the respiratory chain of *Escherichia coli*: An electrochemical and scanning electrochemical microscopy study of the antimicrobial mechanism of micromolar Ag⁺. *Biochemistry* 44(39):13214–13223.
- Kalimuthu K, Suresh Babu R, Venkataraman D, Bilal M, Gurunathan S (2008) Biosynthesis of silver nanocrystals by *Bacillus licheniformis*. *Colloids Surf B Biointerfaces* 65(1):150–153.
- Chatterjee S, Bandyopadhyay A, Sarkar K (2011) Effect of iron oxide and gold nanoparticles on bacterial growth leading towards biological application. *J Nanobiotechnology* 9(1):34.
- Prabhu S, Poulouse EK (2012) Silver nanoparticles: mechanism of antimicrobial action, synthesis, medical applications, and toxicity effects. *Int Nano Lett* 2(1):1–10.
- Singh P, et al. (2015) Biosynthesis, characterization, and antimicrobial applications of silver nanoparticles. *Int J Nanomedicine* 10:2567–2577.
- Klueh U, Wagner V, Kelly S, Johnson A, Bryers JD (2000) Efficacy of silver-coated fabric to prevent bacterial colonization and subsequent device-based biofilm formation. *J Biomed Mater Res* 53(6):621–631.
- Liau SY, Read DC, Pugh WJ, Furr JR, Russell AD (1997) Interaction of silver nitrate with readily identifiable groups: Relationship to the antibacterial action of silver ions. *Letts Appl Microbiol* 25(4):279–283.
- Matsumura Y, Yoshikata K, Kunisaki S, Tsuchido T (2003) Mode of bactericidal action of silver zeolite and its comparison with that of silver nitrate. *Appl Environ Microbiol* 69(7):4278–4281.
- Davies RL, Etris SF (1997) Copper, silver and gold in catalysis. The development and functions of silver in water purification and disease control. *Catal Today* 36(1):107–114.
- Yamanaka M, Hara K, Kudo J (2005) Bactericidal actions of a silver ion solution on *Escherichia coli*, studied by energy-filtering transmission electron microscopy and proteomic analysis. *Appl Environ Microbiol* 71(11):7589–7593.
- Slonczewski JL, Foster JW (2013) Microbial pathogenesis. *Microbiology: An Evolving Science* (W.W. Norton & Company, New York), 3rd International Student Ed, pp 1003–1050.
- Fox CL, Jr, Modak SM (1974) Mechanism of silver sulfadiazine action on burn wound infections. *Antimicrob Agents Chemother* 5(6):582–588.
- Rai M, Yadav A, Gade A (2009) Silver nanoparticles as a new generation of antimicrobials. *Biotechnol Adv* 27(1):76–83.
- Radheshkumar C, Münstedt H (2006) Antimicrobial polymers from polypropylene/silver composites—Ag⁺ release measured by anode stripping voltammetry. *React Funct Polym* 66(7):780–788.
- Pal S, Tak YK, Song JM (2007) Does the antibacterial activity of silver nanoparticles depend on the shape of the nanoparticle? A study of the Gram-negative bacterium *Escherichia coli*. *Appl Environ Microbiol* 73(6):1712–1720.
- Solozio M, Odermatt A (1995) Copper and silver transport by CopB-ATPase in membrane vesicles of *Enterococcus hirae*. *J Biol Chem* 270(16):9217–9221.
- Morones-Ramirez JR, Winkler JA, Spina CS, Collins JJ (2013) Silver enhances antibiotic activity against gram-negative bacteria. *Sci Trans Med* 5(190):190ra181.
- Berenbaum MC (1978) A method for testing for synergy with any number of agents. *J Infect Dis* 137(2):122–130.
- Lambert RJW, Johnston MD, Hanlon GW, Denyer SP (2003) Theory of antimicrobial combinations: Biocide mixtures - synergy or addition? *J Appl Microbiol* 94(4):747–759.
- Denyer SP, Hugo WB, Harding VD (1985) Synergy in preservative combinations. *Int J Pharm* 25(3):245–253.
- Moellering RC, Jr, Weinberg AN (1971) Studies on antibiotic synergism against enterococci. II. Effect of various antibiotics on the uptake of 14 C-labeled streptomycin by enterococci. *J Clin Invest* 50(12):2580–2584.
- Bareham CR, Griswold DE, Calabresi P (1974) Synergism of methotrexate with imuran and with 5-fluorouracil and their effects on hemolysis plaque-forming cell production in the mouse. *Cancer Res* 34(3):571–575.
- Hitchings GH, Elion GB (1963) Chemical suppression of the immune response. *Pharmacol Rev* 15(2):365–405.
- Lambert RJW, Lambert R (2003) A model for the efficacy of combined inhibitors. *J Appl Microbiol* 95(4):734–743.
- Lambert RJW (2001) Advances in disinfection testing and modelling. *J Appl Microbiol* 91(2):351–363.
- Tallarida RJ, Kimmel HL, Holtzman SG (1997) Theory and statistics of detecting synergism between two active drugs: Cocaine and buprenorphine. *Psychopharmacology (Berl)* 133(4):378–382.
- Berenbaum MC (1977) Synergy, additivism and antagonism in immunosuppression. A critical review. *Clin Exp Immunol* 28(1):1–18.
- Chen J, Cesario TC, Rentzepis PM (2014) Rationale and mechanism for the low photoinactivation rate of bacteria in plasma. *Proc Natl Acad Sci USA* 111(1):33–38.
- Atiyeh BS, Costagliola M, Hayek SN, Dibo SA (2007) Effect of silver on burn wound infection control and healing: Review of the literature. *Burns* 33(2):139–148.
- Greulich C, et al. (2012) The toxic effect of silver ions and silver nanoparticles towards bacteria and human cells occurs in the same concentration range. *RSC Advances* 2(17):6981–6987.